

# The Physics Capabilities of $\mu^+\mu^-$ Colliders\*

*The Muon Quartet Collaboration*

V. Barger<sup>a</sup>, M.S. Berger<sup>b</sup>, J.F. Gunion<sup>c</sup>, T. Han<sup>c</sup>

<sup>a</sup>*Physics Department, University of Wisconsin, Madison, WI 53706, USA*

<sup>b</sup>*Physics Department, Indiana University, Bloomington, IN 47405, USA*

<sup>c</sup>*Physics Department, University of California, Davis, CA 95616, USA*

**Abstract.** We summarize the potential of muon colliders to probe fundamental physics.  $W^+W^-$ ,  $t\bar{t}$ , and  $Zh$  threshold measurements could determine masses to precisions  $\Delta M_W = 6$  MeV,  $\Delta m_t = 70$  MeV, and  $\Delta m_h = 45$  MeV, to test electroweak radiative corrections. With  $s$ -channel Higgs production, unique to a muon collider, the Higgs mass could be pinpointed ( $\Delta m_h < 1$  MeV) and its width measured. The other Higgs bosons of supersymmetry can be produced and studied by three methods. If instead the  $WW$  sector turns out to be strongly interacting, a 4 TeV muon collider is ideally suited to its study.

## I INTRODUCTION

In this report we address the exciting physics that could be accomplished at muon colliders in the context of the central physics issue of our time: how is the electroweak symmetry broken, weakly or strongly? Higgs bosons and a low energy supersymmetry (SUSY) are the particles of interest in the weakly broken scenario and new resonances at the TeV scale of a new strong interaction dynamics are the alternatives.

Muon colliders would have decided advantages over other machines in providing (i) sharp beam energy for precision measurements of masses, widths and couplings of the Higgs,  $W$ ,  $t$  and supersymmetry particles, and (ii) high energy / high luminosity for production of high mass particles and studies of a strongly interacting electroweak sector (SEWS).

In order to be able to do interesting physics at a muon collider, the minimum luminosity requirement is

---

\*) Talk presented by V. Barger at the symposium *New Ideas for Particle Accelerators*, Institute for Theoretical Physics, Santa Barbara, California, October 1996.

$$L > \frac{1000 \text{ events/year}}{\sigma_{\text{QED}}}, \quad (1)$$

where  $\sigma_{\text{QED}}$  is the cross section for the process  $\mu^+\mu^- \rightarrow \gamma \rightarrow e^+e^-$ ,

$$\sigma_{\text{QED}} \approx \frac{100 \text{ fb}}{s(\text{TeV})^2}. \quad (2)$$

The prototype designs under consideration well exceed the figure of merit in (1).

- First Muon Collider (FMC)

$$(250 \text{ GeV}) \times (250 \text{ GeV}) \quad \mathcal{L} = 2 \times 10^{33} \text{ cm}^{-2} \text{ s}^{-1} \quad (20 \text{ fb}^{-1}/\text{year}),$$

$$N_{\text{QED}} \approx 8000 \text{ events/year}.$$

- Next Muon Collider (NMC)

$$(2 \text{ TeV}) \times (2 \text{ TeV}) \quad \mathcal{L} = 10^{35} \text{ cm}^{-2} \text{ s}^{-1} \quad (1000 \text{ fb}^{-1}/\text{year}),$$

$$N_{\text{QED}} \approx 6000 \text{ events/year}.$$

Special purpose rings may be added to these designs at modest cost, to optimize luminosities at specific energies for study of  $s$ -channel resonances and thresholds.

Muon colliders offer several unique and highly advantageous features. First,  $s$ -channel Higgs boson production occurs at interesting rates. The Higgs coupling is proportional to the mass, so this process is highly suppressed at  $e^+e^-$  and  $pp$  colliders. Second, a fine energy resolution is an intrinsic property of muon colliders. A beam energy resolution  $R = 0.04$  to  $0.08\%$  is natural and a resolution down to  $R = 0.01\%$  is realizable.<sup>1</sup> By comparison,  $R > 1\%$  is expected at an  $e^+e^-$  machine. The root mean square spread in center-of-mass energy  $\sigma_{\sqrt{s}}$  is given in terms of  $R$  by

$$\sigma_{\sqrt{s}} = (7 \text{ MeV}) \left( \frac{R}{0.01\%} \right) \left( \frac{\sqrt{s}}{100 \text{ GeV}} \right). \quad (3)$$

The monochromaticity of the c.m. energy is *vital* for  $s$ -channel Higgs studies and *valuable* for threshold measurements. Furthermore, for mass measurements a c.m. calibration can be obtained of MeV accuracy, and the necessary energy calibration  $\delta\sqrt{s} \sim 10^{-6}$  may be achieved with spin rotation measurements of polarized muons in the ring. A final, but no less significant aspect of muon colliders, is that their c.m. energy reach is extendable into the  $\sqrt{s} > 1$  TeV range where new physics is expected (either SUSY or SEWS).

## II THRESHOLD PHYSICS AT THE FMC

Precision measurements of  $M_W$  and  $m_t$  can provide important constraints on the Higgs mass in the SM, or other new physics beyond the SM, through the relation

$$M_W = M_Z \left[ 1 - \frac{\pi\alpha}{\sqrt{2} G_\mu M_W^2 (1 - \delta r)} \right]^{1/2}, \quad (4)$$

where the loop contributions  $\delta r$  depend on  $m_t^2$  and  $\log m_h$  in the SM and also on sparticle masses in supersymmetry. The optimal relative precision of  $M_W$  and  $m_t$  measurements is

$$\Delta M_W \approx \frac{1}{140} \Delta m_t, \quad (5)$$

for example  $\Delta M_W \approx 2$  MeV for  $\Delta m_t \approx 200$  MeV.

### A $WW$ and $t\bar{t}$ thresholds<sup>2</sup>

There is excellent potential to make very precise  $M_W$ ,  $m_t$  and  $m_h$  measurements at the FMC because of the sharp beam energy, the suppression of initial state radiation and the absence of significant beamstrahlung. With  $100 \text{ fb}^{-1}$  luminosity just above the  $WW$  threshold ( $\sqrt{s} \approx 161$  GeV) a  $M_W$  precision

$$\Delta M_W = 6 \text{ MeV} \quad (6)$$

is attainable. With  $100 \text{ fb}^{-1}$  devoted to a 10 point scan ( $\sqrt{s} = 1$  GeV) over the  $t\bar{t}$  threshold, the top quark mass could be measured to an accuracy

$$\Delta m_t = 70 \text{ MeV}. \quad (7)$$

Then, with improved determinations of  $\alpha$ ,  $\alpha_s$ , and  $\sin^2 \theta_w$ , such  $M_W$  and  $m_t$  measurements would constrain the SM Higgs to a precision

$$m_{h-0.11m_h}^{+0.13m_h}, \quad (8)$$

(e.g.  $100_{-11}^{+13}$  GeV). The limiting factor on  $\Delta m_h$  is the uncertainty on  $M_W$ . Correspondingly tight constraints would be placed on other new physics. The shape of the  $t\bar{t}$  threshold also constrains  $\alpha_s(M_Z)$ , the top quark width  $\Gamma_t$ , and possibly also  $m_h$  (via  $h$ -exchange contributions).

## B $Zh$ threshold<sup>3</sup>

In the minimal standard model (MSSM), the parameters of the Higgs sector are

$$\tan \beta = \frac{v_2}{v_1} \quad \text{and} \quad m_A \quad (9)$$

at tree level, and also the top-quark and stop masses and stop mixing at the loop level. The light Higgs boson is the only supersymmetric particle with an iron-clad upper bound, which is<sup>4</sup>

$$m_h < 64\text{--}105 \text{ GeV} \quad \text{for } \tan \beta \simeq 1.8, \quad (10)$$

$$m_h < 98\text{--}125 \text{ GeV} \quad \text{for } \tan \beta \simeq 60. \quad (11)$$

Thus it is the first target for experimental searches.

A light Higgs boson will be produced at a lepton collider via the  $Z$ -bremsstrahlung process

$$\ell^+ \ell^- \rightarrow Z^* \rightarrow Zh. \quad (12)$$

With high resolution energy measurements the recoil mass and  $h$ -mass reconstruction give high precision  $m_h$ . With  $50 \text{ fb}^{-1}$  luminosity at a  $\sqrt{s} = 500 \text{ GeV}$   $e^+e^-$  collider, the following precisions are anticipated

$$\Delta m_h = 180 \text{ MeV} \quad (\text{SLD type detector}), \quad (13)$$

$$\Delta m_h = 20 \text{ MeV} \quad (\text{super-JLC detector}). \quad (14)$$

A threshold measurement of the  $Zh$  production cross section provides a new approach to precisely determine  $m_h$ . Figure 1 shows the predicted energy dependence of the cross section. The  $Zb\bar{b}$  background is very small, except in the case when  $m_h \sim M_Z$ . A measurement with  $100 \text{ fb}^{-1}$  luminosity at  $\sqrt{s} = m_h - M_Z + 0.5 \text{ GeV}$  of the cross section at a muon collider would yield a SM Higgs mass to within

$$\Delta m_h = 45 \text{ MeV} \quad (15)$$

for  $m_h = 100 \text{ GeV}$ .

## III $s$ -CHANNEL HIGGS PHYSICS<sup>5</sup>

A unique capability of a muon collider is the production of a Higgs resonance in the  $s$ -channel,  $\mu^+\mu^- \rightarrow h \rightarrow b\bar{b}$ . The light quark background can be rejected by  $b$ -tagging. The resonance cross section is

$$\sigma_h = \frac{4\pi\Gamma(h \rightarrow \mu\bar{\mu})\Gamma(h \rightarrow b\bar{b})}{(s - m_h^2)^2 + m_h^2\Gamma_h^2}. \quad (16)$$

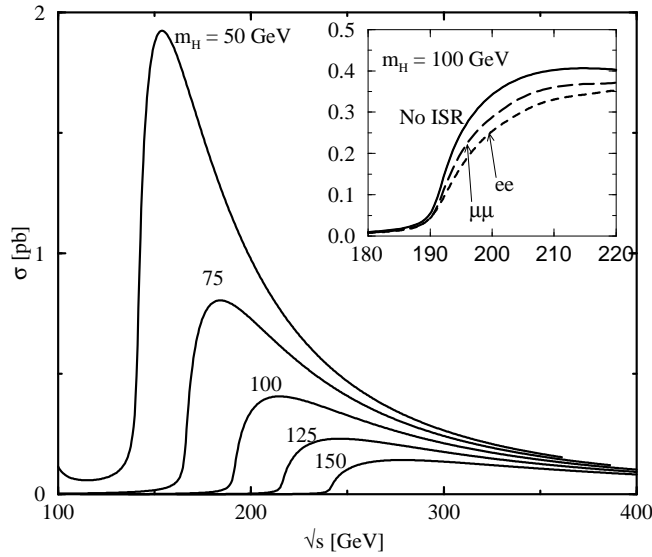


**FIGURE 1.** The cross section vs.  $\sqrt{s}$  for the process  $\ell^+\ell^- \rightarrow Z^*h \rightarrow f\bar{f}h$  for a range of Higgs masses. The inset figure shows the detailed structure for  $m_h = 100$  GeV in the threshold region. Also shown in the inset figure are the effects of initial state radiation (ISR) and beam energy smearing assuming a Gaussian spread  $R_e = 1\%$  for  $e^+e^-$  and  $R_\mu = 0.1\%$  for  $\mu^+\mu^-$ .

One needs to tune the Higgs energy to  $\sqrt{s} = m_h$  by an energy scan in the vicinity of  $m_h$ . The signal is enhanced with polarized beams if the luminosity decrease with polarization<sup>6</sup> is less than  $(1+P)^2/(1-P)^2$  which is 10 for  $P = 0.84$ .

The Higgs resonance profile depends on the total Higgs width,  $\Gamma_h$ , which is highly model dependent. Figure 2 shows expectations for  $\Gamma_h$  in the SM and the MSSM. A light ( $\lesssim 125$  GeV) SM Higgs has a relatively narrow width,  $\Gamma_h \sim$  few MeV. The width of the light Higgs in the MSSM is larger than that of the SM Higgs and scales up roughly with  $(\tan\beta)^2$ . Figure 3 shows the light Higgs resonance profile for the SM Higgs and the MSSM Higgs at  $\tan\beta = 10$  and 20, for resolutions  $R = 0.01\%$ , 0.06% and 0.1%. For a resolution  $\sigma \sim \Gamma_h$ , the Breit-Wigner line shape can be measured and  $\Gamma_h$  determined. To be sensitive to  $\Gamma_h$  of a few MeV, a resolution  $R = 0.01\%$  is needed.

## A Energy scan

An energy scan can be made for a  $s$ -channel Higgs resonance in the mass range  $63 \text{ GeV} < m_h < 2M_W$ . For detection we require a significance  $S/\sqrt{B} > 5$  and assume excellent resolution  $R = 0.01\%$  ( $\sigma_{\sqrt{s}} = 7$  MeV) to assure sensitivity to the narrow width of a SM Higgs. The necessary luminosity per scan point for

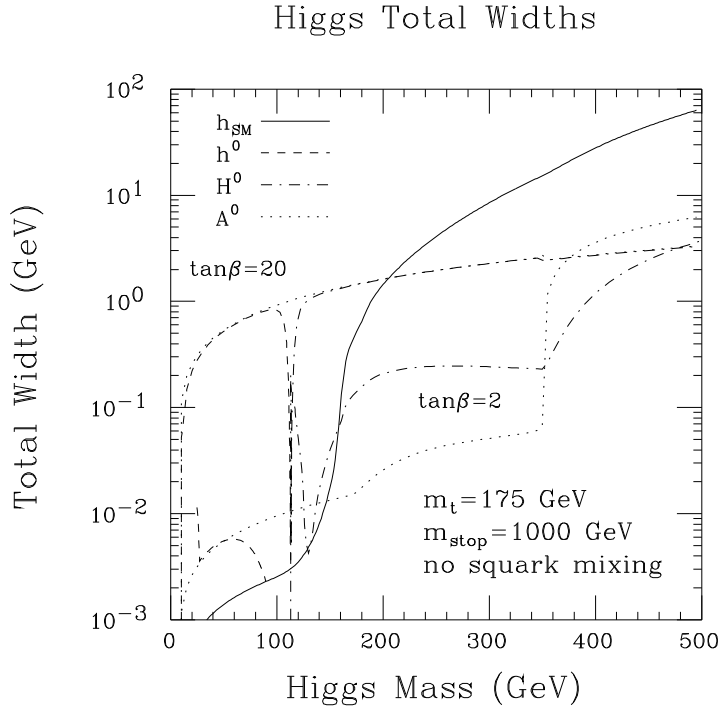


**FIGURE 2.** Total width versus mass of the SM and MSSM Higgs bosons for  $m_t = 175$  GeV. In the case of the MSSM, we have plotted results for  $\tan\beta = 2$  and  $20$ , taking  $m_{\tilde{\tau}} = 1$  TeV and including two-loop radiative corrections, neglecting squark mixing; SUSY decay channels are assumed to be absent.

representative  $m_h$  values is

$L/\text{point}$	$m_h$
$0.01 \text{ fb}^{-1}$	110 GeV
$0.1 \text{ fb}^{-1}$	except near $M_Z$
$1 \text{ fb}^{-1}$	near $M_Z$

The number of scan points needed to zero in on  $m_{h_{\text{SM}}}$  within 1 rms spread  $\sigma_{\sqrt{s}} = 7$  MeV is

$\# \text{ scan points}$	$L_{\text{total}}$	$\delta m_h$
230	$2.3 \text{ fb}^{-1}$	800 MeV (LHC)
3	$0.03 \text{ fb}^{-1}$	20 MeV ( $\ell^+\ell^- \rightarrow Zh$ )

where the right-hand column is the assumed prior knowledge on  $\delta m_h$ .

## B Fine Scan

Once a rough scan has determined the Higgs mass to an accuracy

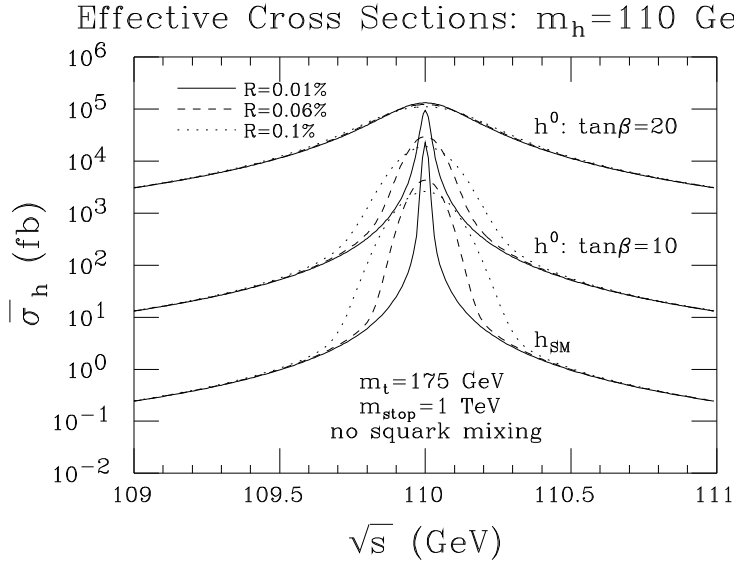


**FIGURE 3.** The effective cross section,  $\bar{\sigma}_h$ , obtained after convoluting  $\sigma_h$  with the Gaussian distributions for  $R = 0.01\%$ ,  $R = 0.06\%$ , and  $R = 0.1\%$ , is plotted as a function of  $\sqrt{s}$  taking  $m_h = 110$  GeV. Results are displayed in the cases:  $h_{SM}$ ,  $h^0$  with  $\tan\beta = 10$ , and  $h^0$  with  $\tan\beta = 20$ . In the MSSM  $h^0$  cases, two-loop/RGE-improved radiative corrections have been included for Higgs masses, mixing angles, and self-couplings assuming  $m_{\tilde{t}} = 1$  TeV and neglecting squark mixing. The effects of bremsstrahlung are not included in this figure.

$$\delta m_h = \sigma_{\sqrt{s}} d \quad \text{with } d \lesssim 0.3 \quad (17)$$

a three-point fine scan can pinpoint the Higgs mass to still higher precision. For this, the optimal distribution of luminosity is  $L$  on the peak location found in the rough scan and  $2.5L$  on each of the resonance wings at  $\pm 2\sigma_{\sqrt{s}}$  from the peak. The measurement of  $\sigma_{\text{wings}}/\sigma_{\text{peak}}$  improves the  $m_h$  precision and measures  $\Gamma_h$ . As an illustration we consider  $m_{h_{SM}} = 110$  GeV for which  $\Gamma_{h_{SM}} = 3$  MeV. Then with a total luminosity  $L_{\text{total}} = 3 \text{ fb}^{-1}$  and a resolution  $R = 0.01\%$ , a fine scan would yield

$$\delta m_h = 0.4 \text{ MeV} \quad \delta \Gamma_h = 1 \text{ MeV}, \quad (18)$$

which is a 30% measurement of the SM Higgs width.

### C $h_{\text{MSSM}}$ or $h_{\text{SM}}$ ?

After the Higgs discovery, the next burning question is whether it is the SM Higgs or the MSSM Higgs boson. There are two ways to know. The first way is to measure  $\Gamma_h$  and  $\Gamma(h \rightarrow \mu\mu) \times B(h \rightarrow \bar{b}b)$ . The couplings of the MSSM Higgs to  $\bar{b}b$  and  $\mu^+\mu^-$  are substantially greater than the SM Higgs coupling to a heavy MSSM Higgs mass of  $m_H \sim 400$  GeV. The two scenarios are thereby distinguishable at the  $3\sigma$  level with  $L = 50 \text{ fb}^{-1}$  and  $R = 0.01\%$ , except for  $m_h$  near  $M_Z$ .

The second way is to find the other heavier MSSM Higgs bosons. At the LHC there are some regions of  $\tan\beta$  vs.  $m_A$  where only the lightest MSSM Higgs boson can be discovered. In the larger  $m_A$  limit of many supergravity models, the masses of  $H^0$ ,  $A^0$ , and  $H^\pm$  are approximately degenerate and  $h$  looks increasingly like  $h_{\text{SM}}$  in its properties. There are 3 possible  $H^0, A^0$  search techniques at muon colliders:

### 1. Scan for $s$ -channel Higgs

With  $L_{\text{total}} = 50 \text{ fb}^{-1}$  the  $H^0, A^0$  discovery prospects are robust for  $250 \text{ GeV} \leq m_{H^0, A^0} \lesssim \sqrt{s}$  and  $\tan\beta \gtrsim 3$ . Overlapping  $H^0, A^0$  resonances can be separated by the scan; see Fig. 4. The  $H^0, A^0$  widths ( $\Gamma \sim 0.1$  to  $0.6 \text{ GeV}$ ) are larger than resolution and can be measured by the scan.

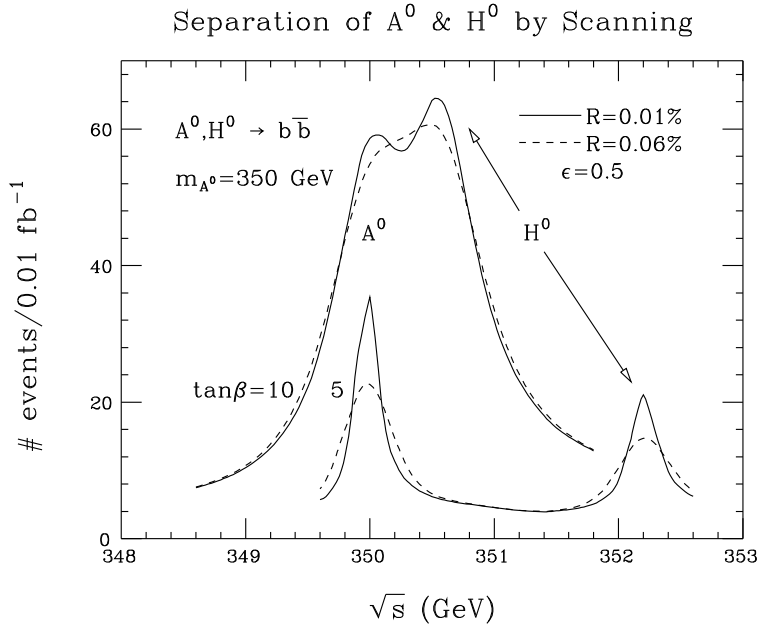


**FIGURE 4.** Plot of  $b\bar{b}$  final state event rate as a function of  $\sqrt{s}$  for  $m_{A^0} = 350 \text{ GeV}$ , in the cases  $\tan\beta = 5$  and  $10$ , resulting from the  $H^0, A^0$  resonances and the  $b\bar{b}$  continuum background. We have taken  $L = 0.01 \text{ fb}^{-1}$  (at any given  $\sqrt{s}$ ), efficiency  $\epsilon = 0.5$ ,  $m_t = 175 \text{ GeV}$ , and included two-loop/RGE-improved radiative corrections to Higgs masses, mixing angles and self-couplings using  $m_{\tilde{t}} = 1 \text{ TeV}$  and neglecting squark mixing. SUSY decays are assumed to be absent. Curves are given for two resolution choices:  $R = 0.01\%$  and  $R = 0.06\%$

### 2. Bremsstrahlung tail

When the muon collider is run at full energy,  $s$ -channel production of  $H^0, A^0$  will result from the luminosity in the bremsstrahlung tail; see Fig. 5. This production is competitive with the scan search for  $\tan\beta \gtrsim 5-7$  and invariant mass resolution  $\Delta M_{b\bar{b}} = \pm 5 \text{ GeV}$ .

### 3. $HA, H^+H^+$ pair production

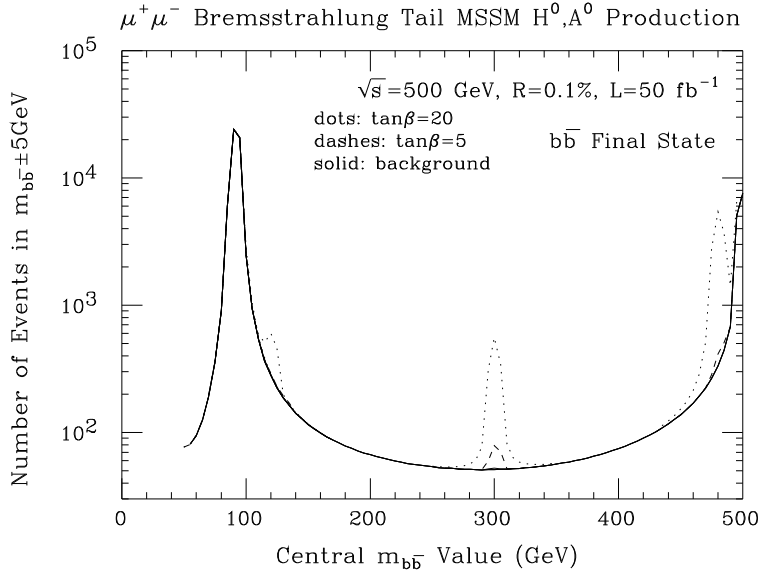


**FIGURE 5.** Taking  $\sqrt{s} = 500$  GeV, integrated luminosity  $L = 50 \text{ fb}^{-1}$ , and  $R = 0.1\%$ , we consider the  $b\bar{b}$  final state and plot the number of events in the interval  $[m_{b\bar{b}} - 5 \text{ GeV}, m_{b\bar{b}} + 5 \text{ GeV}]$ , as a function of the location of the central  $m_{b\bar{b}}$  value, resulting from the low  $\sqrt{\hat{s}}$  bremsstrahlung tail of the luminosity distribution. MSSM Higgs boson  $H^0$  and  $A^0$  resonances are present for the parameter choices of  $m_{A^0} = 120, 300$  and  $480$  GeV, with  $\tan\beta = 5$  and  $20$  in each case. Enhancements for  $m_{A^0} = 120, 300$  and  $480$  GeV are visible for  $\tan\beta = 20$ ;  $\tan\beta = 5$  yields visible enhancements only for  $m_{A^0} = 300$  and  $480$  GeV. Two-loop/RGE-improved radiative corrections are included, taking  $m_t = 175$  GeV,  $m_{\tilde{t}} = 1$  TeV and neglecting squark mixing. SUSY decay channels are assumed to be absent.

At the NMC (4 TeV) the discovery a very heavy Higgs boson is feasible via the the processes  $\mu^+\mu^- \rightarrow Z^* \rightarrow HA, H^+H^+$ . Cross sections are illustrated in Fig. 6. Once discovery is made, special storage rings can be constructed with c.m. energy  $\sqrt{s} \sim m_A, m_H$  to measure the Higgs widths and partial widths.

Note that at the NMC the large event rates for production of the light Higgs boson may allow measurement of rare decay modes there, e.g.  $h \rightarrow \gamma\gamma$ .

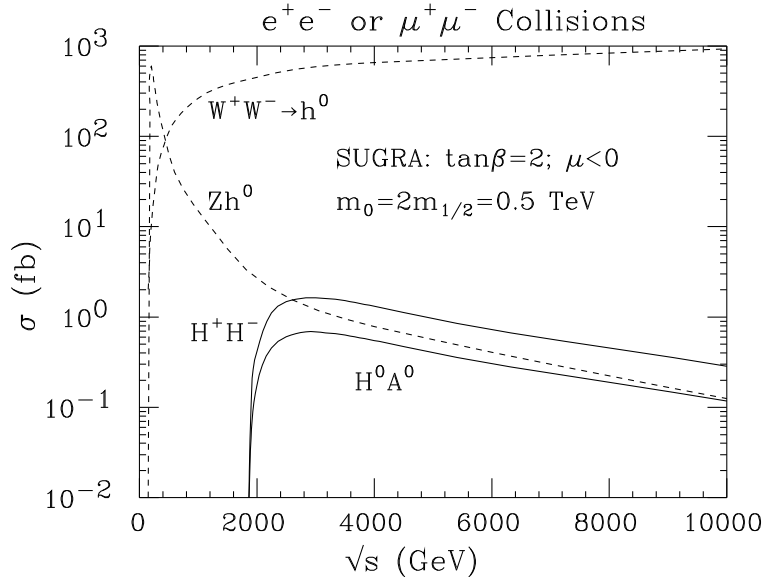


**FIGURE 6.** Pair production of heavy Higgs bosons at a high energy lepton collider. For comparison, cross sections for the lightest Higgs boson production via the Bjorken process  $\mu^+\mu^- \rightarrow Z^* \rightarrow Zh^0$  and via the  $WW$  fusion process are also presented.

## IV ADVANTAGES/NECESSITY OF A HIGH ENERGY MUON COLLIDER

A compelling case for building a 4 TeV NMC exists for both the weakly or strongly interacting electroweak symmetry breaking scenarios.

### A Weakly interacting scenario<sup>7</sup>

Supersymmetry has many scalar particles (sleptons, squarks, Higgs bosons). Some or possibly many of these scalars may have TeV-scale masses. Since spin-0 pair production is  $p$ -wave suppressed at lepton colliders, energies well above the thresholds are *necessary* for sufficient production rates; see Fig. 7. Moreover, the single production mechanisms at lepton colliders and the excellent initial state energy resolution are *advantageous* in reconstructing sparticle mass spectra from their complex cascade decays.

### B Strongly interacting electroweak scenarios (SEWS)<sup>8</sup>

If no Higgs boson exists with  $m_h < 600$  GeV, then partial wave unitarity of  $WW \rightarrow WW$  scattering requires that the scattering be strong at the 1–2 TeV energy scale. The  $WW \rightarrow WW$  scattering amplitude is

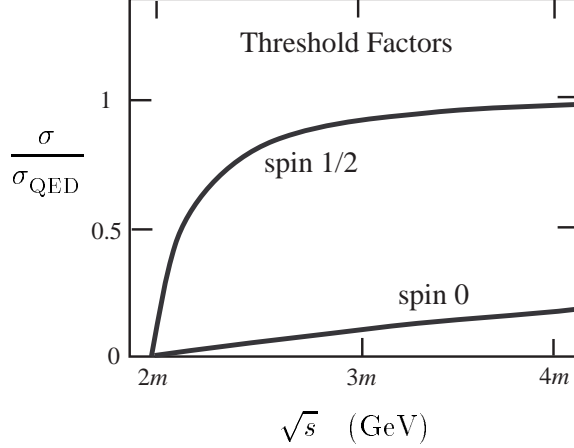


**FIGURE 7.** Comparison of kinematic suppression for fermion pairs and squark pair production at  $e^+e^-$  or  $\mu^+\mu^-$  colliders.

$$A \sim m_H^2/v^2 \quad \text{if light Higgs,} \quad (19)$$

$$\sim s_{WW}/v^2 \quad \text{if no light Higgs.} \quad (20)$$

Then new physics must be manifest at high energies. Energy reach is a critical matter here with subprocess energies  $\sqrt{s_{WW}} \gtrsim 1.5$  TeV needed to probe strong  $WW$  scattering. Since  $E_\mu \sim (3-5)E_W$ , this condition implies

$$\sqrt{s_{\mu\mu}} \sim (3-5)\sqrt{s_{WW}} \gtrsim 4 \text{ TeV.} \quad (21)$$

Thus the NMC would have sufficient energy for study of the SEWS.

The nature of the underlying physics will be revealed by the study of all possible vector boson–vector boson scattering channels, since the sizes of the signals depend on the resonant or non-resonant interactions in the different isospin channels; see Table 1.

**TABLE 1.** Sizes of SEWS signals in vector boson scattering channels: L (large), M (medium), S (small).

final state	resonant scalar ( $H^0$ )	resonant vector ( $\rho_{TC}$ )	non-resonant (LET)
$W_L^+ W_L^-$	L	L	S
$Z_L Z_L$	L	S	M
$W_L^\pm W_L^\pm$	S	M	L
$W_L^\pm Z$	S	L	S

With  $1000 \text{ fb}^{-1}$  per year the NMC will allow comprehensive studies to be made of any SEWS signals. First, the vector resonance signals will be spectacular, as

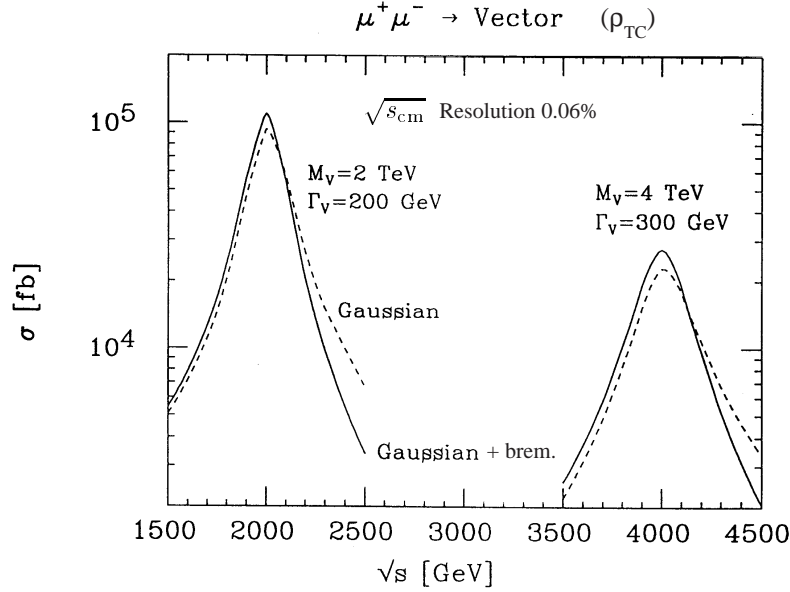


**FIGURE 8.** High event rates are possible if the muon collider energy is set equal to the vector resonance ( $Z'$  or  $\rho_{TC}$ ) mass. Two examples are shown here with  $R = 0.06\%$ .

illustrated in Fig. 8. The production proceeds via vector meson dominance diagrams. On resonance,  $\sqrt{s} \approx M_V$ , the muon collider is a  $V$ -factory. Similarly,  $Z'$  states would also give large signals.<sup>7</sup> Off-resonance production of a vector resonance ( $\sqrt{s} > M_V$ ) can be detected via the bremsstrahlung luminosity. Second, the scalar particle ( $H$ ) signals will be impressive. Figure 9 shows the signal

$$\Delta\sigma = \sigma(m_H = 1 \text{ TeV}) - \sigma(m_H = 0) \quad (22)$$

expected from a 1 TeV scalar resonance. The signal cross sections are

$$\Delta\sigma(WW) = 70 \text{ fb} \quad \text{and} \quad \Delta\sigma(ZZ) = 40 \text{ fb}. \quad (23)$$

Measurements could differentiate scalar models by measuring the resonance width to  $\pm 30$  GeV. Finally, there will be good low energy theorem (LET) signals too.

Angular distributions of the jets in the  $WW \rightarrow 4\text{jet}$  final state will provide a powerful discrimination of SEWS from the light Higgs theory, as illustrated in Fig. 10. Here  $\theta^*$  is the angles of  $q$  and  $\bar{q}$  from  $W$ -decays in  $W$ -rest frames, relative to the  $W$ -boost direction in the  $WW$  c.m. averaged over all configurations.

The  $W_L^+ W_L^- \rightarrow \bar{t}t$  channel is another valuable domain for SEWS studies, since  $W_L^+ W_L^- \rightarrow \bar{t}t$  also violates unitarity at high energies. Figure 11 illustrates expected cross sections.

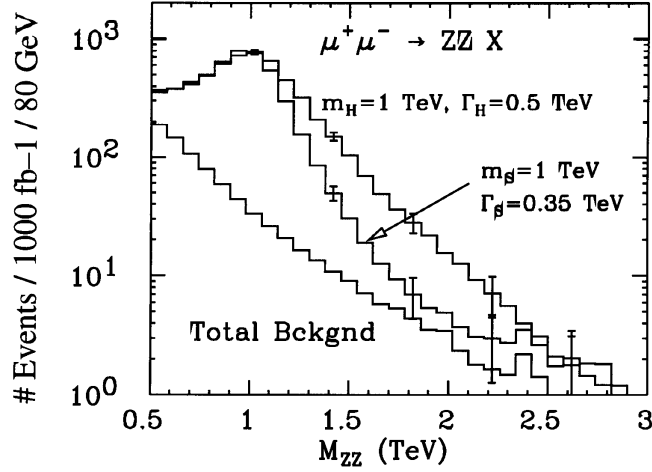


**FIGURE 9.** Events vs.  $M_{VV}$  for two SEWS models (including the combined backgrounds) and for the combined backgrounds alone in the  $ZZ$  final states. Signals shown are: (i) the SM Higgs with  $m_{h_{SM}} = 1$  TeV,  $\Gamma_H = 0.5$  TeV; (ii) the Scalar model with  $M_S = 1$  TeV,  $\Gamma_S = 0.35$  TeV. Results are for  $L = 1000$  fb $^{-1}$  and  $\sqrt{s} = 4$  TeV. Sample error bars are shown at  $M_{VV} = 1.02, 1.42, 1.82, 2.22$  and  $2.62$  TeV for the illustrated 80 GeV bins. Results are for  $L = 1000$  fb $^{-1}$  and  $\sqrt{s} = 4$  TeV.

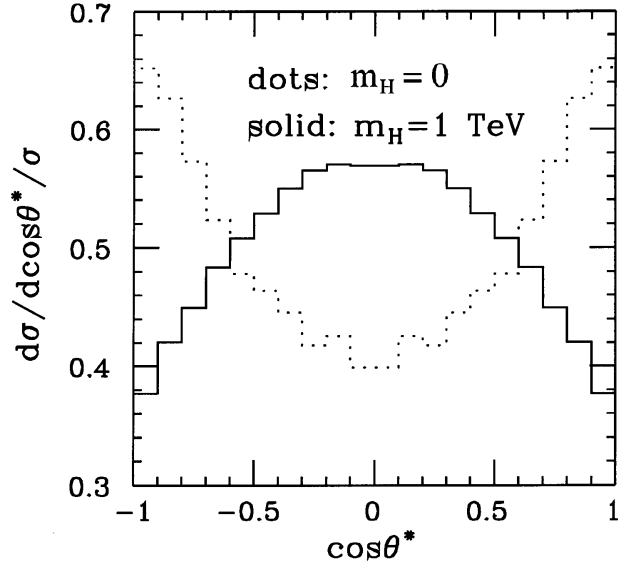


**FIGURE 10.** Plot of normalized cross section shapes and  $dN/d\cos\theta^*$  (for  $L = 200$  fb $^{-1}$ ) as a function of the  $\cos\theta^*$  of the  $W^+$  decays in the  $W^+W^+$  final state. Error bars for a typical  $dN/d\cos\theta^*$  bin are displayed. For this plot we require  $M_{VV} \geq 500$  GeV,  $p_T^V \geq 150$  GeV,  $|\cos\theta_W^{\text{lab}}| < 0.8$  and  $30 \leq p_T^{VV} \leq 300$  GeV.

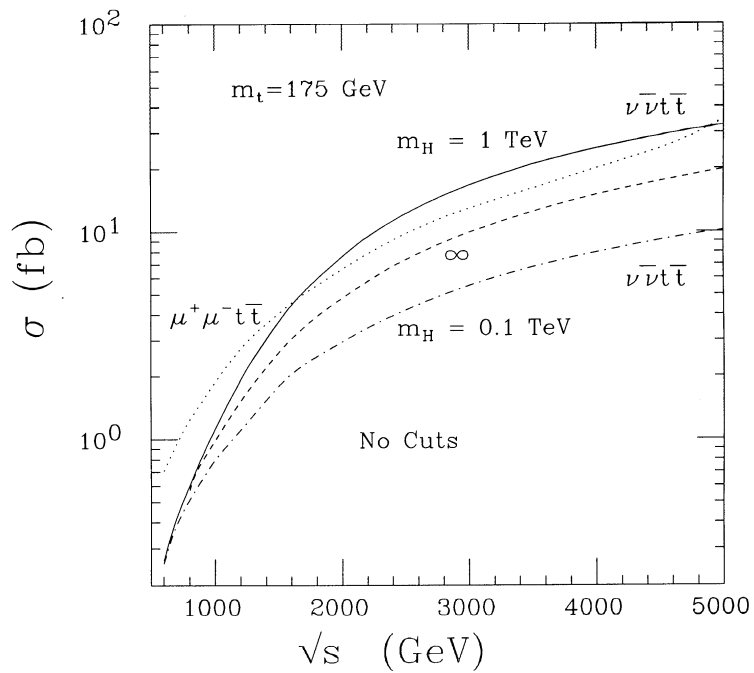


**FIGURE 11.** Cross section vs.  $\sqrt{s}$  for  $\mu^+\mu^- \rightarrow \nu\bar{\nu}t\bar{t}$ ,  $\mu^+\mu^-t\bar{t}$  for Higgs masses  $m_H = 0.1$  TeV, 1 TeV, and  $\infty$ .

## V CONCLUSION

In summary, muon colliders are a natural match to the physics of electroweak symmetry breaking. The sharp muon beam energy allows

- precision threshold measurements of  $M_W, m_t, m_h$  to test electroweak radiative corrections.
- $s$ -channel resonance scans to precisely determine  $m_h$  and measure  $\Gamma_h$ .
- discovery and study of the heavy MSSM Higgs bosons in 3 ways.

The NMC provides the c.m. energy and luminosity for

- heavy supersymmetry thresholds, or
- SEWS studies.

If the  $WW$  sector proves to be strongly interacting, the NMC is ideally suited to probe the nature of these new interactions.

## ACKNOWLEDGEMENTS

This research was supported in part by the U.S. Department of Energy under Grant No. DE-FG02-95ER40896 and in part by the University of Wisconsin Research Committee with funds granted by the Wisconsin Alumni Research Foundation.

## REFERENCES

1. R.B. Palmer, private communication; G.P. Jackson and D. Neuffer, private communication.
2. V. Barger, M.S. Berger, J.F. Gunion, and T. Han, Univ. of Wisconsin-Madison report MADPH-96-963 (1996).
3. V. Barger, M.S. Berger, J.F. Gunion, and T. Han, Univ. of Wisconsin-Madison preprint MADPH-96-979 (1996).
4. See e.g. M. Carena, J.R. Espinosa, M. Quiros, and C.E.M. Wagner, *Phys. Lett.* **B355**, 209 (1995).
5. V. Barger, M.S. Berger, J.F. Gunion, and T. Han, *Phys. Rev. Lett.* **75**, 1462 (1995); V. Barger, M.S. Berger, J.F. Gunion, and T. Han, Univ. of Wisconsin-Madison report MADPH-96-930 (1996), to appear in *Physics Reports*.
6. See, for example, Z. Parsa,  *$\mu^+\mu^-$  Collider and Physics Possibilities*, unpublished.
7. V. Barger, M.S. Berger, J.F. Gunion, and T. Han, *Proceedings of the Symposium on Physics Potential and Development of  $\mu^+\mu^-$  Colliders*, San Francisco, CA, 1995, ed. by D. Cline and D. Sanders, *Nucl. Phys. B (Proc. Suppl.)* **51A**, 13 (1996).
8. V. Barger, M.S. Berger, J.F. Gunion, and T. Han, *Phys. Rev.* **D55**, 142 (1997).